Autonomous Robots 3, 269–283 (1996)

A Dynamic Model of an Underwater Vehicle with a Robotic Manipulator using Kane's Method

T.J. TARN, G.A. SHOULTS AND S.P. YANG
Department of Systems Science and Mathematics, Campus Box 1040, Washington University, St. Louis, MO 63130, USA

Abstract. Development of a robust autonomous Underwater Robotic Vehicle (URV) is a key element to the exploitation of marine resources. An accurate dynamic model is important for both controller design and mission simulation, regardless of the control strategy employed. In this paper, a dynamic model for an underwater vehicle with an n-axis robot arm is developed based on Kane's method. The technique provides a direct method for incorporating external environmental forces into the model. The model developed in this paper includes four major hydrodynamic forces: added mass, profile drag, fluid acceleration, and buoyancy. The model derived is a closed form solution which can be utilized in modern model-based control schemes.

Keywords: underwater robotic vehicle, hydrodynamic forces, thruster dynamic model, Kane's method

1. Introduction

An Underwater Robotic Vehicle can greatly enhance the capabilities for oceanic engineering including oil and mineral explorations, inspection, and construction. However, control strategies for URV are still immature compared with their space based counterparts. Part of the reason is that we still don't have a precise model for an URV. The difficulty arises from the high density, complex, unstructured ocean environment. The dynamics for a fixed land based manipulator are well understood, and can easily be developed using either the Euler-Lagrange or Newton-Euler iteration method (Craig, 1989). However, development of a model for an underwater robotic vehicle has met with limited success, primarily as a result of the uncertainties presented by the hydrodynamic forces. Many control schemes have been proposed for underwater vehicles (Nakamura and Savant, 1992; Goheen and Jefferys, 1990; Yoerger and Slotine, 1985). In Nakamura and Savant (1992), a controller is developed for a six degree-of-freedom (DOF) underwater vehicle for the purpose of trajectory tracking. The model is developed in the velocity frame, and utilizes control inputs for linear and angular velocity to achieve trajectory tracking. The model is applied to kinematic motion control of the vehicle only, and does not include dynamics, or address the control of a manipulator. In Goheen and Jefferys (1990), a controller is investigated as an autopilot for underwater vehicles with the intent of performing autoposition and station-holding. This is a difficult problem using a conventional autopilot control scheme because of the lack of a precise model and the uncertainties presented by the unstructured hydrodynamic environment. Two multivariable self-tuning controller designs are presented as an approach to overcome model uncertainties. The equations of motion used in Goheen and Jefferys (1990), are derived from conventional testing techniques. The vehicle is mounted in a Planar Motion Mechanism (PMM) which oscillates the vehicle in a prescribed manner. Through different tests with each oscillatory mode, and varying PMM oscillatory frequencies and carriage speed, a pair of hydrodynamic coefficients are derived. Such a technique is very time consuming and expensive and requires a prototype vehicle. In Yoerger and Slotine (1985), a sliding mode control for a single input is proposed for robust trajectory control. No parameters of the model are known exactly. These control schemes (Goheen and Jefferys, 1990; Yoerger and

Slotine, 1985) claim that good performance can still be achieved without precisely knowing the model parameters. These methods use a variety of techniques that perform system identification either explicitly or implicitly.

Better performance can certainly be achieved with a more detailed model. Modeling methods for underwater vehicles fall into two major categories (Goheen, 1991): design methods which are concerned with the calculation of a proposed vehicle's dynamic motion parameters from the vehicle's design information; and testing techniques that require experimental data from a prototype vehicle from which the equations of motion are derived. The design method gives more physical meaning, but may not be as accurate as testing techniques. However, development of a prototype vehicle and the use of an experimental facility may be cost prohibitive.

One purpose for designing an underwater vehicle is to carry a manipulator and perform station-keeping while the manipulator performs work. Once a manipulator arm becomes attached to the underwater vehicle, it becomes a multibody hydrodynamic problem. There has been a lot of current research addressing the multibody hydrodynamics problem which can be found in Mahesh et al. (1991), Ioi and Itoh (1990), McMillan et al. (1995), Kato and Lane (1995). In Mahesh et al. (1991), an underwater vehicle equipped with a manipulator is described. A coordinated control scheme is developed which controls the vehicle and manipulator simultaneously and compensates the end-effector error resulting from motion of the vehicle. The model is developed using an NBOD2 approach which derives the equations of motion for the N-coupled rigid bodies which form a topological tree. The control system is based on a discrete-time approximation of the dynamic model. The model of the robot used in the paper is planar. In Ioi and Itoh (1990), the author expands the classic Newton-Euler mechanics to formulate the dynamic model of an underwater manipulator. McMillan et al. (1995) develop a dynamic simulation algorithm based on the Articulated-Body dynamics for an unmanned underwater vehicle with a robotic manipulator. These dynamic models, which are developed with the Newton-Euler method, result in a set of dynamic equations presented in recursion form, which are valuable for simulation, but less useful from a control standpoint.

Our main consideration for underwater robotic manipulator modeling include: (1) successful operation of an autonomous URV, which dictates a model-based dynamic control system; (2) requiring accurate modeling of both the manipulator and vehicle; and (3) requiring accurate modeling of the interaction of the dynamic system with the underwater environment. An alternative technique satisfying these model requirements for an underwater robotic manipulator is presented here using Kane's method (Kane et al., 1983). The technique uses generalized speeds, partial angular and linear velocities to formulate expressions for generalized forces in a particularly effective way and enables one to construct, with a minimum of labor, equations of motion having the simplest form possible. The final model derived in this paper is in a closed form. Since modern control theory is based on the state space formulation, the closed form model enables us to recast our model into the state space form. This will allow us to use the results obtained in modern control theory. Especially to investigate the structural properties of the model, such as controllability, observability, identifiability, decoupling theory, tracking theory and stability. Therefore, the closed form model will deepen our understanding of the model which in turn will improve the operation, safety, and reliability of the URV.

2. Kane's Dynamical Equations

2.1. Advantage of Kane's Method

Euler-Lagrange (E-L) and Newton-Euler (N-E) are among the two most commonly used modeling methods. The E-L method eliminates interaction forces between adjacent links and provides a systematic method for developing the equations of motion of the entire system. A drawback of the E-L method is that it involves many unnecessary computations associated with developing an energy function (Lagrangian) of the system. The N-E method is a recursive formulation which involves solving a force balance equation for each link in the system. Link interaction forces are incorporated into constraint equations which must be computed, although they do not produce any work on the system. Although the method reduces to a relatively simple set of recursive equation, the constraint equations associated with the link interaction forces can become computationally expensive, especially if the links form a closed kinematic loop. Kane's method is in some sense a combination of the E-L and N-E methods. Like the E-L method, Kane's method eliminates the non-working link interaction forces from the

onset, and considers the whole system as a single entity. Kane's method requires that one develop the generalized active forces and generalized inertia forces for each link in the system. These forces are developed using N-E type equations, while eliminating the non-working constraint forces. These equations are another form of the Gibbs-Appell equations, or generalized D'Alembert equations written in Lagrangian form. In essence, Kane's dynamical equations are equivalent to a set of "n" independent E-L equations, where "n" is the degree of freedom of the system (Angeles et al., 1989). Kane's method is more direct in that it eliminates the link interaction forces associated with the N-E method and eliminates the need to develop an energy or Gibbs function associated with the E-L method.

2.2. *Kane's Equations*

Given a system S possessing N degrees of freedom in a Newtonian frame, let $\dot{q}_1, \ldots, \dot{q}_N$ be the N generalized speeds for S. Let $\mathbf{F}_1 \ldots, \mathbf{F}_N$, be the generalized active forces for S, and $\mathbf{F}_1^*, \ldots, \mathbf{F}_N^*$, be the generalized inertia forces associated with S. Then all motions of S are governed by the equations (Kane et al., 1983):

$$\mathbf{F}_r + \mathbf{F}_r^* = 0 \quad (r = 1, \ldots, N). \tag{1}$$

If a set of contact and/or body forces acting on a rigid body B belonging to S is equivalent to a torque $\mathbf{T}$, together with a force $\mathbf{R}$ applied at a point Q of B, then $(\mathbf{F}_r)_B$, the contribution of this set of forces to $\mathbf{F}_r$, is given by:

$$(\mathbf{F}_r)_B = \omega_r \cdot \mathbf{T} + v_{Q_r} \cdot \mathbf{R} \quad (r = 1, \ldots, N), \tag{2}$$

where, ω_r and v_{Q_r} are respectively, the rth partial angular velocity of B, and the rth partial linear velocity of Q. The rth partial angular velocity of B, ω_r, is defined as:

$$\omega_r \equiv \frac{\partial \omega}{\partial \dot{q}_r}, \tag{3}$$

where, ω is the angular velocity about the center of mass of B. The rth partial linear velocity, v_{Q_r}, of Q is defined similarly as:

$$v_{Q_r} \equiv \frac{\partial \mathbf{v}_Q}{\partial \dot{q}_r}, \tag{4}$$

where $\mathbf{v}_Q$ is the linear velocity of Q. The contribution to $\mathbf{F}_r^*$ of all inertia forces for the particles of a rigid body B belonging to S, is given by the following:

$$(\mathbf{F}_r^*)_B = \omega_r \cdot \mathbf{T}^* + v_r \cdot \mathbf{R}^* \quad (r = 1, \ldots, N), \tag{5}$$

where, v_r is the rth partial linear velocity of the center of mass of B, and $\mathbf{R}^*$ and $\mathbf{T}^*$ are respectively the inertia force and torque of B. The inertial force of B is defined as:

$$\mathbf{R}^* \equiv -m\mathbf{a}, \tag{6}$$

where, m is the mass of B, and $\mathbf{a}$ is the acceleration of the center of mass of B. The inertia torque of B is defined as:

$$\mathbf{T}^* \equiv -\alpha \cdot \mathbf{I} - \omega \times \mathbf{I} \cdot \omega, \tag{7}$$

where, $\mathbf{I}$, is the central inertia matrix of B, and ω and α are the angular velocity and acceleration of B.

3. URV Model

In this section we will develop a dynamic model for an URV. The task involves applying the equations presented in Section 2 to a system composed of an n link manipulator arm attached to an underwater vehicle. The technique requires that we develop expressions for the generalized inertia forces for the vehicle and the n links of the system, and expressions for all of the generalized active forces which act on the vehicle and the manipulator.

3.1. *Coordinate System*

The kinematic task is more tractable and systematic if we exploit the use of Denavit-Hartenberg (D-H) coordinate frames. Figure 1, illustrates the coordinates that we have selected for our system, where we have attached a fixed 0th coordinate frame to the vehicle which we treat as a zeroth link in an $n + 1$ link system. The 0th frame is located with respect to the center-of-mass (C.M.) of the vehicle (or Link 0) by the vector $\mathbf{c}_0^0 = [c_{x_0}\ c_{y_0}\ c_{z_0}\ 1]^t$, where the subscript indicates Link 0, the superscript indicates a vector expressed in the 0th coordinate frame, and "t" denotes transpose. We have also carried along a 4th coordinate, 1, to be consistent with a homogeneous coordinate system. Development of the equations of motion also dictate the establishment of an inertial coordinate system, of

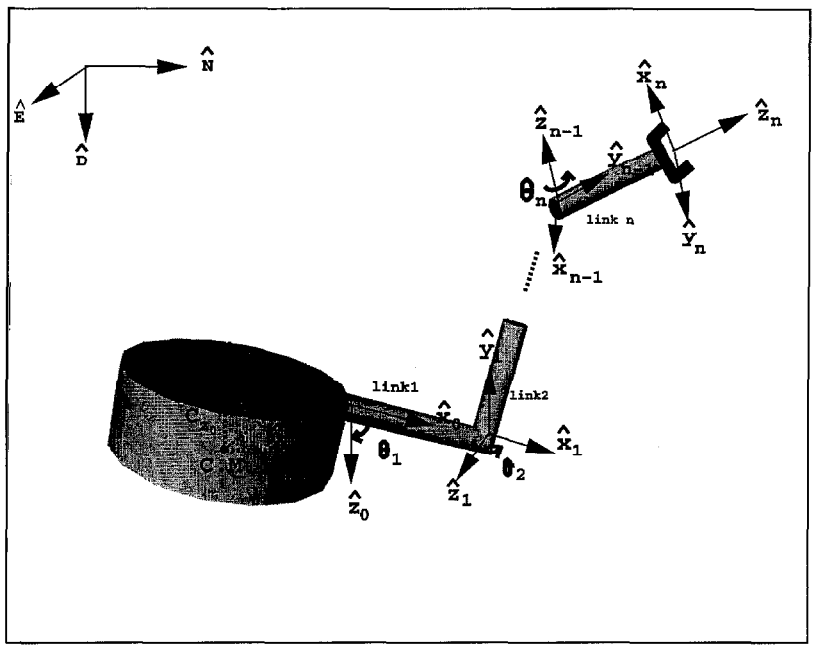

Figure 1. Coordinate system for URV model.

which we have chosen a local level North, East, Down (NED) coordinate system. We will select the $N = n+6$ generalized speeds of the system as:

$$\dot{\mathbf{q}} = [\, v_x \quad v_y \quad v_z \quad \omega_x \quad \omega_y \quad \omega_z \quad \dot{\theta}_1, \ldots, \dot{\theta}_n]^t,$$

where, $(v_x,\ v_y,\ v_z)$ is the linear velocity of the vehicle with respect to the inertial NED frame expressed in the 0th coordinate frame, $(\omega_x,\ \omega_y,\ \omega_z)$ is the angular velocity of the vehicle with respect to the inertial NED frame expressed in the 0th coordinate frame, and $(\dot{\theta}_1, \ldots, \dot{\theta}_n)$ which are the joint speeds of the n link manipulator arm. The kinematic expressions and inertia forces are simpler if represented in the moving 0th coordinate frame. Thus, all force expressions, as well as all derivatives and dot products will be performed in the 0th coordinate frame. Unless stated otherwise, superscripts on vectors denote the vector basis, and subscripts pertain to a particular link in the system.

3.2. *Kinematic Analysis*

In this section we will develop expressions for the linear and angular velocities, and linear and angular accelerations for each link. For simplicity we have considered only revolute links, but the notation could easily be expanded to include prismatic links.

Position Vector of C.M. of Link j. The position vector of the C.M. of Link 1, with respect to the C.M. of the vehicle (Link 0) expressed in the 0th coordinate frame is given by:

$$\mathbf{p}_1^0 = \begin{bmatrix} c_{x_0} \\ c_{y_0} \\ c_{z_0} \\ 1 \end{bmatrix} \tilde{+} \mathbf{A}_0^1 \mathbf{c}_1^1 = \mathbf{c}_0^0 \tilde{+} \mathbf{A}_0^1 \mathbf{c}_1^1,$$

where, $\tilde{+}$ denote the addition of the physical coordinates of the two homogeneous vectors on the right hand side, $\mathbf{A}_0^1$ is the homogeneous transformation from coordinate frame 1 to coordinate frame 0, and $\mathbf{c}_1^1$ is the position vector to the C.M. of Link 1 expressed in frame 1. The position vector of the C.M. of Link 2 with respect to the C.M. of the vehicle is given similarly by:

$$\mathbf{p}_2^0 = \mathbf{c}_0^0 \tilde{+} \mathbf{A}_0^1 \mathbf{A}_1^2 \mathbf{c}_2^2,$$

and for an arbitrary Link j, $j = 1, \ldots, n$, by the following:

$$\mathbf{p}_j^0 = \mathbf{c}_0^0 \tilde{+} \prod_{k=1}^{j} \mathbf{A}_{k-1}^k \mathbf{c}_j^j, \tag{8}$$

where, $\mathbf{c}_j^j = [c_{x_j}\ c_{y_j}\ c_{z_j}\ 1]^t$ is the homogeneous position vector of the C.M. of Link j, expressed in the jth frame.

The angular velocity of the vehicle with respect to an inertial frame, expressed in the 0th coordinate system is given by:

$$ {}^{i}\omega^{0} = \omega_x \hat{x}_0 + \omega_y \hat{y}_0 + \omega_z \hat{z}_0, $$

where, the hat "$\wedge$" denotes a unit vector, and the notation ${}^{t}\omega^{s}$ denotes the angular velocity of frame s with respect to frame t expressed in the 0th coordinate frame. The angular velocity of an arbitrary Link j, with respect to the inertial NED frame expressed in the 0th coordinate frame is given by:

$$ \begin{aligned} {}^{i}\omega^{1} &= {}^{i}\omega^{0} + {}^{0}\omega^{1} = {}^{i}\omega^{0} + \dot{\theta}_z \hat{z}_0 && \text{(Link 1)}, \\ {}^{i}\omega^{2} &= {}^{i}\omega^{0} + {}^{0}\omega^{1} + \bar{\mathbf{A}}_0^1 \, {}^{1}\omega^{2} \\ &= {}^{i}\omega^{0} + \dot{\theta}_1 \hat{z}_0 + \bar{\mathbf{A}}_0^1 \dot{\theta}_2 \hat{z}_1 && \text{(Link 2)}, \\ &\vdots \\ {}^{i}\omega^{j} &= {}^{i}\omega^{0} + {}^{0}\omega^{1} + \sum_{l=1}^{j-1} \prod_{m=1}^{l} \bar{\mathbf{A}}_{m-1}^{m} \, {}^{l}\omega^{l+1} && \text{(Link } j\text{)}, \end{aligned} \tag{9} $$

where, $\bar{\mathbf{A}}_j^i$ denotes the rotation submatrix of $\mathbf{A}_j^i$, ${}^{l}\omega^{l+1} = [0 \; 0 \; \dot{\theta}_{l+1}]^t$ is the angular velocity of Link $l+1$ with respect to Link l, expressed in the lth coordinate frame.

Linear Velocity of the C.M. of Link j. The linear velocity of the C.M. of the vehicle with respect to the inertial NED frame, expressed in the 0th coordinate system is given by:

$$ \mathbf{v}_0^0 = v_x \hat{x}_0 + v_y \hat{y}_0 + v_z \hat{z}_0. $$

The linear velocity of the C.M. of an arbitrary Link j, with respect to the inertial NED frame, expressed in the 0th coordinate frame is given by:

$$ \begin{aligned} \mathbf{v}_1^0 &= \mathbf{v}_0^0 + \frac{d\mathbf{p}_1^0}{dt} + {}^{i}\omega^{0} \times \mathbf{p}_1^0 && \text{(Link 1)}, \\ \mathbf{v}_2^0 &= \mathbf{v}_0^0 + \frac{d\mathbf{p}_2^0}{dt} + {}^{i}\omega^{0} \times \mathbf{p}_2^0 && \text{(Link 2)}, \\ &\vdots \\ \mathbf{v}_j^0 &= \mathbf{v}_0^0 + \frac{d\mathbf{p}_j^0}{dt} + {}^{i}\omega^{0} \times \mathbf{p}_j^0 && \text{(Link } j\text{)}. \end{aligned} \tag{10} $$

Angular Acceleration of Link j. The angular acceleration about the C.M. of the vehicle with respect to the inertial NED frame, expressed in the 0th coordinate frame is given by:

$$ {}^{i}\alpha^{0} = \frac{d^{i}\omega^{0}}{dt} = \dot{\omega}_x \hat{x}_0 + \dot{\omega}_y \hat{y}_0 + \dot{\omega}_z \hat{z}_0. $$

The angular acceleration of an arbitrary Link j, with respect to the inertial NED frame expressed in the 0th coordinate frame is found from the following:

$$ \begin{aligned} {}^{i}\alpha^{1} &= \frac{d^{i}\omega^{1}}{dt} + {}^{i}\omega^{0} \times {}^{i}\omega^{1} && \text{(Link 1)}, \\ {}^{i}\alpha^{2} &= \frac{d^{i}\omega^{2}}{dt} + {}^{i}\omega^{0} \times {}^{i}\omega^{2} && \text{(Link 2)}, \\ &\vdots \\ {}^{i}\alpha^{j} &= \frac{d^{i}\omega^{j}}{dt} + {}^{i}\omega^{0} \times {}^{i}\omega^{j} && \text{(Link } j\text{)}. \end{aligned} \tag{11} $$

Linear Acceleration of the C.M. of Link j. The linear acceleration of the C.M. of the vehicle with respect to the inertial NED frame, expressed in the 0th coordinate frame is given by:

$$ \mathbf{a}_0^0 = \frac{d\mathbf{v}_0^0}{dt} + {}^{i}\omega^{0} \times \mathbf{v}_0^0. $$

The linear acceleration of the C.M. of an arbitrary Link j, with respect to the inertial NED frame expressed in the 0th coordinate frame is found similarly by the following:

$$ \begin{aligned} \mathbf{a}_1^0 &= \frac{d\mathbf{v}_1^0}{dt} + {}^{i}\omega^{0} \times \mathbf{v}_1^0 && \text{(Link 1)}, \\ \mathbf{a}_2^0 &= \frac{d\mathbf{v}_2^0}{dt} + {}^{i}\omega^{0} \times \mathbf{v}_2^0 && \text{(Link 2)}, \\ &\vdots \\ \mathbf{a}_j^0 &= \frac{d\mathbf{v}_j^0}{dt} + {}^{i}\omega^{0} \times \mathbf{v}_j^0 && \text{(Link } j\text{)}. \end{aligned} \tag{12} $$

3.3. *Inertia Forces*

The generalized inertia force of the system requires that we develop expressions for the inertia force and torque of each link in the system. The inertia force of an arbitrary Link j, is given by the following:

$$ \mathbf{R}_j^* = -m_j \mathbf{a}_j^0, $$

where, m_j is the mass of Link j, and $\mathbf{a}_j^0$ is the linear acceleration of the C.M. of Link j, and is given by

Eq. (12). The inertia torque of an arbitrary Link j, is given by the following:

$$\mathbf{T}_j^* = -\mathbf{I}_j^0 \cdot {}^i\alpha^j - {}^i\omega^j \times \mathbf{I}_j^0 \cdot {}^i\omega^j,$$

where, $\mathbf{I}_j^0$, is the central inertia matrix of Link j, expressed in the 0th coordinate frame. $\mathbf{I}_j^0$ is found through the following similarity transformation:

$$\mathbf{I}_j^0 = \bar{\mathbf{A}}_0^j \mathbf{I}_j^j (\bar{\mathbf{A}}_0^j)^t,$$

where, $\mathbf{I}_j^j$ the central inertia matrix of Link j, expressed in the jth coordinate frame, and $\bar{\mathbf{A}}_0^j$ is the rotation submatrix of the $\mathbf{A}_0^j$ relating frame j with the 0th coordinate frame. The generalized inertia force for the system is now found using Eqs. (5)–(7) to obtain the following:

$$\mathbf{F}_r^* = \sum_{j=0}^{n} \left(\frac{\partial {}^i\omega^j}{\partial \dot{q}_r} \cdot \mathbf{T}_j^* + \frac{\partial \mathbf{v}_j^0}{\partial \dot{q}_r} \cdot \mathbf{R}_j^* \right) \quad (r = 1, \ldots, N). \tag{13}$$

3.4. *Gravity Forces*

Gravity can be treated as a generalized active force which acts at the center of mass of each link in the system. The force due to gravity acting on an arbitrary Link j is given by:

$$\mathbf{R}_{\text{grav}_j} = m_j \mathbf{g}^0,$$

where, $\mathbf{g}^0 = [g_x \; g_y \; g_z]^T$, is the gravity vector expressed in the 0th coordinate frame. The generalized active force due to gravity is found from Eq. (2) and is given by the following:

$$(\mathbf{F}_r)_{\text{gravity}} = \sum_{j=0}^{n} m_j \frac{\partial \mathbf{v}_j^0}{\partial \dot{q}_r} \cdot \mathbf{g}^0 \quad (r = 1, \ldots, N). \tag{14}$$

3.5. *Hydrodynamic Forces*

The hydrodynamic forces induced by the motion of a rigid body in an underwater environment are very complex and highly nonlinear. A general discussion of hydrodynamic forces and their impact on submerged bodies can be found in Yuh (1995), Fossen (1994), Patel (1989). The forces may be developed using incompressible fluid flow using Navior-Stokes equation, and rarely lead to a closed form solution. As is often the case, these forces may be treated as lumped approximations for certain applications within certain underlying assumptions. Previous work by Yuh (1990), identified four separate effects which must be included in a dynamic simulation of a submerged rigid body. The net effect of added mass, buoyancy, fluid acceleration, and drag are often treated as the superposition of each individual force. The next 4 sub-sections will describe each hydrodynamic force, and will develop a general formulation for incorporating that force into our URV dynamic model.

Added Mass. The added mass force results from the interaction of fluid in the immediate vicinity of a submerged link which is accelerating relative to the fluid. The link induces an acceleration on the fluid through a pressure distribution which acts on the link body. The force required to accelerate the surrounding fluid results in an effective inertia which can be modeled with a 6×6 positive definite added mass inertia matrix, $\mathbf{I}_A$. For a completely submerged vehicle in an unbounded fluid the added mass coefficients may be treated as constants. Analytic expressions for the coefficients of $\mathbf{I}_A$ can be derived from potential flow theory for simple geometric shapes (Fossen, 1994; Patel, 1989). In general the 36 elements of the added mass matrix, $\mathbf{I}_A$, for a body in a real fluid would be distinct and may be determined from experimental testing techniques. It has been shown by McMillan et al. (1995) and can be derived from Fossen (1994), that the inertia force and torque of a submerged body induced by the added mass phenomena has the following form:

$$\begin{bmatrix} \mathbf{R}_{A_j}^* \\ \mathbf{T}_{A_j}^* \end{bmatrix} = -\mathbf{I}_{A_j}^0 \begin{bmatrix} \dot{\mathbf{v}}_j^0 \\ {}^i\dot{\omega}^j \end{bmatrix} - \begin{bmatrix} {}^i\tilde{\omega}^j & 0 \\ \tilde{\mathbf{v}}_j^0 & {}^i\tilde{\omega}^j \end{bmatrix} \mathbf{I}_{A_j}^0 \begin{bmatrix} \mathbf{v}_j^0 \\ {}^i\omega^j \end{bmatrix}, \tag{15}$$

where, ${}^i\tilde{\omega}^j$ and $\tilde{\mathbf{v}}_j^0$ are skew symmetric matrices, and $\mathbf{I}_{A_j}^0$ is the 6×6 added mass matrix for Link j expressed in the 0th coordinate frame. $\dot{\mathbf{v}}_j^0$ is the time derivative of Link j in the moving 0th frame and is given by Eq. (12):

$$\dot{\mathbf{v}}_j^0 = \mathbf{a}_j^0 - {}^i\omega^0 \times \mathbf{v}_j^0,$$

and ${}^i\dot{\omega}^j$ is the time derivative of ${}^i\omega^j$ in the moving 0th frame and is given by Eq. (11):

$${}^i\dot{\omega}^j = {}^i\alpha^j - {}^i\omega^0 \times {}^i\omega^j.$$

Substituting these two equations into Eq. (15) results in:

$$\begin{bmatrix} \mathbf{R}^*_{A_j} \\ \mathbf{T}^*_{A_j} \end{bmatrix} = -\mathbf{I}^0_{A_j} \begin{bmatrix} \mathbf{a}^0_j \\ {}^i\alpha^j \end{bmatrix} + \mathbf{I}^0_{A_j} \begin{bmatrix} {}^i\omega^j \times \mathbf{v}^0_j \\ {}^i\omega^0 \times {}^i\omega^j \end{bmatrix} - \begin{bmatrix} {}^i\tilde{\omega}^j & 0 \\ \tilde{\mathbf{v}}^0_j & {}^i\tilde{\omega}^j \end{bmatrix} \mathbf{I}^0_{A_j} \begin{bmatrix} \mathbf{v}^0_j \\ {}^i\omega^j \end{bmatrix}. \quad (16)$$

We can account for the relative acceleration and velocity of the fluid by introducing the following relationship:

$$v^0_j = \mathbf{v}^0_j - \mathbf{v}^0_f,$$
$$a^0_j = \mathbf{a}^0_j - \mathbf{a}^0_f,$$

where, $\mathbf{v}^0_f$ is the velocity of the fluid expressed in the 0th coordinate frame, and $\mathbf{a}^0_f$ is the acceleration of the fluid expressed in the 0th coordinate frame. The final form of the inertia force and torque resulting from added mass is now given by:

$$\begin{bmatrix} \mathbf{R}^*_{A_j} \\ \mathbf{T}^*_{A_j} \end{bmatrix} = -\mathbf{I}^0_{A_j} \begin{bmatrix} a^0_j \\ {}^i\alpha^j \end{bmatrix} + \mathbf{I}^0_{A_j} \begin{bmatrix} {}^i\omega^j \times v^0_j \\ {}^i\omega^0 \times {}^i\omega^j \end{bmatrix} - \begin{bmatrix} {}^i\tilde{\omega}^j & 0 \\ \tilde{v}^0_j & {}^i\tilde{\omega}^j \end{bmatrix} \mathbf{I}^0_{A_j} \begin{bmatrix} v^0_j \\ {}^i\omega^j \end{bmatrix}. \quad (17)$$

The generalized inertia force due to the added mass for the entire system is then given by the following:

$$(\mathbf{F}^*_r)_{\text{AM}} = \sum_{j=0}^{n} \left(\frac{\partial {}^i\omega^j}{\partial \dot{q}_r} \cdot \mathbf{T}^*_{A_j} + \frac{\partial \mathbf{v}^0_j}{\partial \dot{q}_r} \cdot \mathbf{R}^*_{A_j} \right) \quad (r = 1, \ldots, N). \quad (18)$$

This is a general formulation for the incorporation of the hydrodynamic force and torque into the dynamic model. No assumptions were necessary on how the coefficients of the added mass matrix are derived.

Buoyancy. The buoyancy force is proportional to the mass of the fluid displaced by the link and acts through the center of buoyancy of the link. For a homogeneous symmetric shape, the center of buoyancy and center of mass are equivalent. For our model, we assume that the buoyancy force acts through the center of mass of the link and is given by the following:

$$\mathbf{R}_{B_j} = -\rho V_j \mathbf{g}^0,$$

where, ρ is the density of the fluid, V_j is the volume of fluid displaced by Link j, and $\mathbf{g}^0$ is the gravity vector expressed in the 0th coordinate frame. The generalized active force due to buoyancy for the system is given by the following:

$$(\mathbf{F}_r)_{\text{Buoy}} = -\rho \sum_{j=0}^{n} V_j \frac{\partial \mathbf{v}^0_j}{\partial \dot{q}_r} \cdot \mathbf{g}^0 \quad (r = 1, \ldots, N). \quad (19)$$

Fluid Acceleration. The fluid acceleration force is similar to the buoyancy force in that it is proportional to the fluid displaced, but is result of acceleration of the fluid itself. The force due to fluid acceleration also acts through the center of buoyancy and is given by:

$$\mathbf{R}_{Fl_j} = \rho V_j \mathbf{a}^0_f,$$

where, again, $\mathbf{a}^0_f$ is the acceleration of the fluid expressed in the 0th coordinate frame. The generalized active force due to fluid acceleration for the system is given by the following:

$$(\mathbf{F}_r)_{\text{Fluid Accel}} = \rho \sum_{j=0}^{n} V_j \frac{\partial \mathbf{v}^0_j}{\partial \dot{q}_r} \cdot \mathbf{a}^0_f \quad (r = 1, \ldots, N). \quad (20)$$

Profile Drag. The fluid drag forces exerted on a body depends on the square of the relative velocity of the fluid with respect to the body; the geometric shape of the body which is characterized by a drag coefficient and a reference area of the body; and the density of the fluid. The drag forces include profile (pressure) drag, skin friction drag, and lift forces. The profile drag force acts in a direction opposite to the link relative velocity with respect to the fluid and is the primary drag force for slow moving URV applications. Both skin friction drag which is tangent to the link surface and lift which is normal to the fluid flow may be neglected for slow moving URV applications. Therefore, we will only consider profile drag in our formulation. However, the other drag forces could be handled for other applications in an analogous manor. The profile drag force on an infinitesimal part of the link is given by L'evesque and Richard (1994):

$$d\mathbf{R}_{\text{Drag}_j} = -0.5\rho C_D b_j \| v^0_j(l)^{\perp} \| v^0_j(l)^{\perp} dl,$$

$$d\mathbf{T}_{\text{Drag}_j} = -0.5\rho C_D b_j \| v^0_j(l)^{\perp} \| (\bar{\mathbf{A}}^j_0 l \hat{x}_j \times v^0_j(l)^{\perp}) dl,$$

where, $b_j dl$ is the reference area of Link j, b_j is the width of the rectangle that circumscribes the frontal

projection of the infinitesimal element of Link j, and dl is the length of the infinitesimal element. C_D is the drag coefficient , and $v_j^0(l)^\perp$ is the relative velocity of Link j with respect to the fluid normal to the link along the length, l, of the link. $v_j^0(l)$ is equal to $\mathbf{v}_j^0(l) - \mathbf{v}_f^0$, the velocity of Link j minus the velocity of the fluid. The drag coefficient C_D is a function of link geometry and fluid flow angle. It can be represented by:

$$C_D = C_{D,\text{basic}} \sin^2\sigma,$$

where, $C_{D,\text{basic}}$ is shape parameter, and σ is the angle between the relative velocity of the fluid and the link longitudinal axis. Different values of $C_{D,\text{basic}}$ are suggested in L'evesque and Richard (1994) for different link shapes. Using strip theory, the surface integral can be reduced to a line integral to obtain the following equations for the force and moment on Link j due to profile drag:

$$\begin{aligned}\mathbf{R}_{\text{Drag}_j} &= -0.5\rho \int_0^L \|v_j^0(l)^\perp\| v_j^0(l)^\perp C_D b_j dl,\\ \mathbf{T}_{\text{Drag}_j} &= -0.5\rho \int_0^L \|v_j^0(l)^\perp\| \left(\bar{\mathbf{A}}_0^j l\hat{x}_j \times v_j^0(l)^\perp\right)\\ &\quad \times C_D b_j dl.\end{aligned} \tag{21}$$

The generalized active force due to the drag force and torque for the system is then given by:

$$(\mathbf{F}_r)_{\text{Drag}} = \sum_{j=0}^{n} \left(\frac{\partial^i \omega^j}{\partial \dot{q}_r} \cdot \mathbf{T}_{\text{Drag}_j} + \frac{\partial \mathbf{v}_j^0}{\partial \dot{q}_r} \cdot \mathbf{R}_{\text{Drag}_j} \right) \qquad (r = 1, \ldots, N). \tag{22}$$

3.6. *Control Forces and Thruster Dynamic Model*

Control Forces. To make this model complete, we will consider a control input for each of the N generalized speeds. The vehicle or zeroth link requires 6 control inputs: 3 rotational, and 3 linear. The rotational and linear control inputs for the vehicle can be expressed by the following control vectors:

$$\begin{aligned}\mathbf{T}_0 &= T_x\hat{x}_0 + T_y\hat{y}_0 + T_z\hat{z}_0 \qquad \text{(Rotational)},\\ \mathbf{R}_0 &= R_x\hat{x}_0 + R_y\hat{y}_0 + R_z\hat{z}_0 \qquad \text{(Linear)},\end{aligned}$$

where, T_x, T_y, T_z are the control torques applied about the vehicle C.M., and R_x, R_y, R_z are the control forces applied through the vehicle C.M. parallel to the $\hat{x}_0$, $\hat{y}_0$, $\hat{z}_0$ axes. The n joint controls for the manipulator can be expressed for an arbitrary Link j by the following control vector:

$$\mathbf{T}_j = T_j\hat{z}_{j-1} \qquad \text{(Link } j\text{)},$$

The generalized active force for all of the control inputs of the system is then found from Eq. (2):

$$(\mathbf{F}_r)_{\text{control}} = \frac{\partial^i \omega^0}{\partial \dot{q}_r} \cdot \mathbf{T}_0 + \frac{\partial \mathbf{v}_j^0}{\partial \dot{q}_r} \cdot \mathbf{R}_0 + \frac{\partial^i \omega^1}{\partial \dot{q}_r} \cdot \mathbf{T}_1 + \sum_{j=2}^{n} \frac{\partial^i \omega^j}{\partial \dot{q}_r} \cdot \left(\prod_{m=1}^{j-1} \bar{\mathbf{A}}_{m-1}^m \right) \mathbf{T}_j. \tag{23}$$

The desired control forces $\mathbf{R}_0$ and torques $\mathbf{T}_0$ for the vehicle can be physically implemented by thrusters. Most small-to-medium-sized underwater vehicles are powered by electric motors driving propellers mounted in ducts. Current thruster technology exhibits nonlinearities and limit cycles which can dominate the control problem. Therefore, in order to ensure adequate tracking between commanded and actual thruster inputs, it requires incorporation of the thruster dynamics into the control model.

Thruster Dynamic Model. A good treatment of thruster dynamic models for underwater vehicles can be found in Yuh and Gonugunta (1993), Yoerger et al. (1990), Healey et al. (1994). Yoerger et al. point out in their paper (Yoerger, 1990) that the dynamics of the underwater vehicle can be greatly influenced by the vehicle thruster dynamics. They propose a nonlinear parametric model for a torque-controlled thruster. Three different controller designs were tested for improving the performance of the thrusters. The lumped parameter dynamic model derived in their paper uses an energy-based physical system approach. Using the propeller angular velocity Ω as the state, the thruster dynamic model and output equation are given by the following:

$$\begin{aligned}\dot{\Omega} &= \beta_{\text{th}}\tau_{\text{th}} - \alpha_{\text{th}}\Omega|\Omega|,\\ \text{Thrust} &= C_{\text{th}}\Omega|\Omega|,\end{aligned}$$

where τ_{th} is the input torque for the thruster, α_{th} and β_{th} are constant model parameters, and C_{th} is a proportionality constant. All three constants can be determined through experiments. This model assumes

that the water velocity is directly proportional to the propeller speed resulting in a constant slip angle. A better model which accounts for fluid slip was derived by Healey et al. (1994). Their model includes three parts: motor model, propeller map, and fluid model. These three components are combined into a two state thruster dynamics model give by the following:

$$\dot{\Omega} = g_1(\Omega, v_p, V_s),$$

and

$$\dot{v}_p = g_2(\Omega, v_p),$$

where the propeller angular velocity, Ω, and axial fluid velocity at the propeller v_p are the state variables, and V_s is the voltage input. The thruster output equation is a nonlinear function of the two states and can be expressed by:

$$\text{Thrust} = h(\Omega, v_p).$$

All of the parameters in this model can be identified through experimental analysis. The required thruster forces commands $\text{Thrust}_{\text{com}}$ related to the desired control forces $\mathbf{R}_0$ and torques $\mathbf{T}_0$ for the vehicle can be represented by:

$$\begin{bmatrix} \mathbf{R}_0 \\ \mathbf{T}_0 \end{bmatrix} = \Theta \text{Thrust}_{\text{com}},$$

where Θ is the thruster matrix map that maps the thruster forces to the C.M. of the vehicle in the 0th frame. The commanded thrust input can be obtained by inverting the above relation, taking a pseudo-inverse if necessary.

3.7. *Dynamic Model*

Having developed all of the generalized inertia forces and generalized active forces for the vehicle and manipulator, the equations of motion are found by combining Eqs. (13), (14), and (18)–(23) with Eq. (1) to obtain the following dynamic model:

$$(\mathbf{F}_r^*) + (\mathbf{F}_r^*)_{\text{AM}} + (\mathbf{F}_r)_{\text{gravity}} + (\mathbf{F}_r)_{\text{Buoy}} + (\mathbf{F}_r)_{\text{FluidAccel}} + (\mathbf{F}_r)_{\text{Drag}} + (\mathbf{F}_r)_{\text{control}} = \mathbf{0} \quad (r = 1, \ldots, N). \tag{24}$$

However, Eq. (24) may not be the most convenient form for the equations of motion. A considerable amount of previous research in robotics has resulted in a rather standard form for the equations of motion of a manipulator. Also a considerable amount of previously developed simulation software depends on equations of motion expressed in the following form:

$$\mathbf{M}(\boldsymbol{\xi})\ddot{\mathbf{q}} + \mathbf{C}(\boldsymbol{\xi}, \dot{\mathbf{q}}) + \mathbf{G}(\boldsymbol{\xi}) + \mathbf{F}_{\text{external}} = \tau_{\text{control}}, \tag{25}$$

where, $\boldsymbol{\xi}$ is the joint variable vector, $\mathbf{M}(\boldsymbol{\xi})$ is a matrix of inertia terms, $\mathbf{C}(\boldsymbol{\xi}, \dot{\mathbf{q}})$ is a vector of Coriolis and centripetal accelerations, $\mathbf{G}(\boldsymbol{\xi})$ is a vector of gravity effects, $\mathbf{F}_{\text{external}}$ is a vector of external forces acting on the system, and τ_{control} is a vector of control inputs. Equation (24) can be rearranged into the standardized form in (25) by noting that:

$$\begin{aligned}
(\mathbf{M}(\boldsymbol{\xi}))_{i,j} &= -\partial((\mathbf{F}_i^*) + (\mathbf{F}_i^*)_{\text{AM}})/\partial\ddot{q}_j, \\
(\mathbf{C}(\boldsymbol{\xi}, \dot{\mathbf{q}})) &= -((\mathbf{F}^*) + (\mathbf{F}^*)_{\text{AM}}) - \mathbf{M}(\boldsymbol{\xi})\ddot{\mathbf{q}}, \\
\mathbf{G}(\boldsymbol{\xi}) &= -(\mathbf{F})_{\text{gravity}}, \\
(\mathbf{F}_{\text{external}}) &= -(\mathbf{F})_{\text{Buoy}} - (\mathbf{F})_{\text{Fluid Accel}} - (\mathbf{F})_{\text{Drag}}, \\
(\tau_{\text{control}}) &= (\mathbf{F})_{\text{control}}.
\end{aligned}$$

The dynamic model is now complete, with Eq. (25) representing the equations of motion of the entire system composed of the vehicle and the n-axis manipulator. The output equation relating the position and orientation of the manipulator end-effector in the inertial NED coordinate system takes on the following form:

$$\mathbf{y} = h(\boldsymbol{\xi}, \eta), \tag{26}$$

where, η is the position and orientation vector in the NED coordinate frame, and $h(\boldsymbol{\xi}, \eta)$ is a six dimensional function of the generalized coordinates and is obtained from the following homogeneous transformation relating the manipulator end-effector to the inertial NED coordinate frame.

$$\mathbf{A}_i^n = \mathbf{A}_i^0 \mathbf{A}_0^1 \mathbf{A}_1^2 \cdots \mathbf{A}_{n-1}^n. \tag{27}$$

The n homogeneous transformations which relate the manipulator end-effector to the vehicle frame $(\mathbf{A}_0^1 \mathbf{A}_1^2 \cdots A_{n-1}^n)$ are determined from the Denavit-Hartenberg parameters, which are based on the link shape and joint angle. The displacement and orientation of the vehicle in the inertial NED coordinate frame is represented by the final homogeneous transformation, $\mathbf{A}_i^0$. A convenient set of angles which can be used to describe the vehicle orientation are given by the roll, pitch, and yaw Euler angles (ϕ, θ, ψ). The final homogeneous transformation in terms of Euler angles

takes on the following form, $\mathbf{A}_i^0$,

$$\begin{bmatrix} c\psi c\theta & c\psi s\phi s\theta - c\phi s\psi & c\phi c\psi s\theta + s\phi s\psi & d_n \\ c\theta s\psi & s\phi s\psi s\theta + c\phi c\psi & c\phi s\psi s\theta - c\psi s\phi & d_e \\ -s\theta & c\theta s\phi & c\phi c\theta & d_d \\ 0 & 0 & 0 & 1 \end{bmatrix}, \tag{28}$$

where, $c\theta = \cos(\theta)$, $s\theta = \sin(\theta)$, and $[d_n\ d_e\ d_d]^T$ is the North, East, Down displacement of the vehicle.

For fixed land based manipulators, the position and orientation of the manipulator end-effector is computed from measured joint angles. For underwater robotic vehicles, the position of the manipulator end-effector is determined by not only the manipulator joint angles, but also the position and orientation of the vehicle. Measuring the position and orientation of the vehicle is referred to as "vehicle navigation," and is an area for further research. However, from a simulation standpoint, the manipulator joint angles and vehicle position and orientation can be computed by integrating Eq. (25). The joint angles are available as a direct result of integrating the n joint speeds. The Euler angles, which define the vehicle orientation in the NED frame, can be computed by integrating Euler angle rates. The Euler angle rates in terms of the vehicle angular velocity $(\omega_x,\ \omega_y,\ \omega_z)$ is given by:

$$\begin{bmatrix} \dot{\phi} \\ \dot{\theta} \\ \dot{\psi} \end{bmatrix} = \begin{bmatrix} 1 & \sin\phi\tan\theta & \cos\phi\tan\theta \\ 0 & \cos\theta & -\sin\phi \\ 0 & \sin\phi\sec\theta & \cos\phi\sec\theta \end{bmatrix} \begin{bmatrix} \omega_x \\ \omega_y \\ \omega_z \end{bmatrix}. \tag{29}$$

Although Eq. (29) provides a convenient kinematic relation for computing the Euler angles, it does contain singularities at $\pm 90°$ degrees pitch. A better choice of kinematic variables are quaternions, which do not involve singularities.

4. Example 6 DOF URV with a 3 Link Manipulator

To demonstrate the utility of our modeling approach, we have developed the equations of motion for a generic 6 DOF vehicle with a 3 link Puma 560 manipulator. The vehicle is generic in the sense that the vehicle mass, inertia, and hydrodynamic parameters may be specified at run time (i.e., simulation input parameters). Although, the Puma 560 manipulator is certainly not suitable for underwater manipulation, we chose it as an example to demonstrate the modeling approach and because we have detailed modeling data about the Puma 560 at our disposal. All of the modeling equations outlined in Section 3 were computed using the Mathematica (Wolfram Research Inc.) symbolic computation package on a Sun sparcstation, which performed all of the algebra and derivative operations on symbolic equations. Mathematica has a feature that allows it to output its result in either C or FORTRAN source code. Thus, we are able to generate elements for a dynamic simulation directly from the equations outlined in Section 3, without the need of performing hand computations which greatly reduces the possibility for human error. The results from sample computations will be provided in the following sections. A complete listing of the C source code for the model elements will be provided in the appendix.[1]

4.1. *Coordinate System*

Once again, the inertial coordinate system will be a locally level North, East, Down system. We will attach a 0th coordinate system to the vehicle ($\hat{x}_0$ forward, $\hat{y}_0$ out the left, $\hat{z}_0$ up). We will assume symmetry about the vehicle xz plane, so that the vehicle C.M. is located by the following homogeneous vector:

$$\mathbf{c}_0^0 = [c_{x_0},\ 0,\ c_{z_0},\ 1]^t.$$

The 9 generalized speeds of the system will be defined as:

$$\dot{\mathbf{q}} = [\ v_x\ \ v_y\ \ v_z\ \ \omega_x\ \ \omega_y\ \ \omega_z\ \ \dot{q}_1\ \ \dot{q}_2\ \ \dot{q}_3\ ]^t,$$

where, $(v_x,\ v_y,\ v_z)$ is the inertial velocity of the vehicle expressed in the moving 0th coordinate frame, $(\omega_x,\ \omega_y,\ \omega_z)$ is the angular velocity of the vehicle with respect to the inertial NED frame expressed in the 0th coordinate frame,and $(\dot{q}_1\ \dot{q}_2\ \dot{q}_3)$ are the joint speeds of the Puma 560 manipulator arm.

4.2. *Kinematic Analysis of Example Model*

The first 3 homogeneous transformations for the Puma 560 are given by the following and are detailed in

[Technical report SSM-RL-91-15] (Tarn et al., 1991):

$$A_0^1 = \begin{bmatrix} C_1 & 0 & -S_1 & 0 \\ S_1 & 0 & C_1 & 0 \\ 0 & -1 & 0 & 0 \\ 0 & 0 & 0 & 1 \end{bmatrix},$$

$$A_1^2 = \begin{bmatrix} C_2 & -S_2 & 0 & 0.4318C_2 \\ S_2 & C_2 & 0 & 0.4318S_2 \\ 0 & 0 & 1 & 0 \\ 0 & 0 & 0 & 1 \end{bmatrix},$$

$$A_2^3 = \begin{bmatrix} C_3 & 0 & S_3 & -0.0191C_3 \\ S_3 & 0 & -C_3 & -0.0191S_3 \\ 0 & 1 & 0 & 0.1505 \\ 0 & 0 & 0 & 1 \end{bmatrix},$$

where, C_j means $\mathrm{Cos}(q_j)$, S_j means $\mathrm{Sin}(q_j)$, q_j is the joint angle between Link j and $j-1$, and all measurements are in meters.

The homogeneous vectors defining the C.M. of the first 3 links of the Puma 560 are given by:

$$c_1^1 = [0.0000,\ 0.3088,\ 0.0389,\ 1]^t,$$
$$c_2^2 = [-0.3289,\ 0.0050,\ 0.2038,\ 1]^t,$$
$$c_3^3 = [0.0204,\ 0.0137,\ 0.0037,\ 1]^t.$$

The position vector to the C.M. of each link can now be computed from (8), (e.g. Link 1):

$$p_1^0 = \left[c_{x_0} - 0.0389\ \sin(q_1), 0.0389\ \cos(q_1), -0.3088 + c_{z_0}\ \right]^t.$$

The angular and linear velocities of the links may now be computed from (9) and (10). An example computation from Mathematica for Link 1 is given:

$${}^i\omega^1 = [\omega_x, \omega_y, \omega_z + \dot{q}_1]^t,$$

$$\begin{aligned} v_1^0 = \big[& v_x + \left(-0.3088 + c_{z_0}\right)\omega_y - 0.0389\ \cos(q_1)\,\omega_z \\ & - 0.0389\ \cos(q_1)\,\dot{q}_1, \\ & v_y - \left(-0.3088 + c_{z_0}\right)\omega_x \\ & + \left(c_{x_0} - 0.0389\ \sin(q_1)\right)\omega_z \\ & - 0.0389\ \sin(q_1)\,\dot{q}_1, \\ & v_z + 0.0389\ \cos(q_1)\,\omega_x \\ & - \left(c_{x_0} - 0.0389\ \sin(q_1)\right)\omega_y \big]^t. \end{aligned}$$

The angular and linear accelerations may be computed from Eqs. (11) and (12). The result for Link 1 is given by:

$$\begin{aligned} {}^i\alpha^1 = [& -(\omega_y\omega_z) + \omega_y\,(\omega_z + \dot{q}_1) + \dot{\omega}_x, \\ & \times \omega_x\omega_z - \omega_x\,(\omega_z + \dot{q}_1) + \dot{\omega}_y, \dot{\omega}_z + \ddot{q}_1]^t, \end{aligned}$$

$$\begin{aligned} \mathbf{a}_1^0 = \big[& \omega_y\big(v_z + 0.0389\cos(q_1)\omega_x \\ & - \left(c_{x_0} - 0.0389\sin(q_1)\right)\omega_y\big) \\ & + 0.0389\sin(q_1)\omega_z\dot{q}_1 + 0.0389\sin(q_1)\dot{q}_1^2 \\ & - \omega_z\big(v_y - \left(-0.3088 + c_{z_0}\right)\omega_x \\ & + \left(c_{x_0} - 0.0389\sin(q_1)\right)\omega_z - 0.0389\sin(q_1)\dot{q}_1\big) \\ & + \dot{v}_x + \left(-0.3088 + c_{z_0}\right)\dot{\omega}_y - 0.0389\cos(q_1)\dot{\omega}_z \\ & - 0.0389\cos(q_1)\ddot{q}_1, \\ & - \big(\omega_x\big(v_z + 0.0389\cos(q_1)\omega_x \\ & - \left(c_{x_0} - 0.0389\sin(q_1)\right)\omega_y\big) \\ & - 0.0389\cos(q_1)\omega_z\,\dot{q}_1 - 0.0389\cos(q_1)\dot{q}_1^2 \\ & + \omega_z\big(v_x + \left(-0.3088 + c_{z_0}\right)\omega_y \\ & - 0.0389\cos(q_1)\omega_z - 0.0389\cos(q_1)\dot{q}_1\big) \\ & + \dot{v}_y - \left(-0.3088 + c_{z_0}\right)\dot{\omega}_x \\ & + \left(c_{x_0} - 0.0389\sin(q_1)\right)\dot{\omega}_z - 0.0389\sin(q_1)\ddot{q}_1, \\ & - 0.0389\sin(q_1)\omega_x\dot{q}_1 + 0.0389\cos(q_1)\omega_y\dot{q}_1 \\ & - \omega_y\big(v_x + \left(-0.3088 + c_{z_0}\right)\omega_y \\ & - 0.0389\cos(q_1)\omega_z - 0.0389\cos(q_1)\dot{q}_1\big) \\ & + \omega_x\big(v_y - \left(-0.3088 + c_{z_0}\right)\omega_x \\ & + \left(c_{x_0} - 0.0389\sin(q_1)\right)\omega_z - 0.0389\sin(q_1)\dot{q}_1\big) \\ & + \dot{v}_z + 0.0389\cos(q_1)\dot{\omega}_x \\ & - \left(c_{x_0} - 0.0389\sin(q_1)\right)\dot{\omega}_y\big]^t. \end{aligned}$$

4.3. *Inertia Forces for Example Model*

As previously stated, the vehicle will be modeled with generic mass properties having a mass, m_0, and we will assume that the vehicle principle axes are aligned with the 0th coordinate system so that we have a diagonal inertia matrix:

$$\mathbf{I}_0^0 = \begin{bmatrix} I_{0xx} & 0 & 0 \\ 0 & I_{0yy} & 0 \\ 0 & 0 & I_{0zz} \end{bmatrix} (kg - m^2).$$

The mass and central principle inertia parameters for the first 3 links of the Puma 560 are given by the

following:

$$m1 = 12.96(kg)$$

$$I_1^1 = \begin{bmatrix} 1.09809 & 0 & 0 \\ 0 & 0.177381 & 0 \\ 0 & 0 & 1.1112 \end{bmatrix} (kg - m^2),$$

$$m2 = 22.37(kg)$$

$$I_2^2 = \begin{bmatrix} 0.403567 & 0 & 0 \\ 0 & 0.968405 & 0 \\ 0 & 0 & 0.966379 \end{bmatrix} (kg - m^2),$$

$$m3 = 5.01(kg)$$

$$I_3^3 = \begin{bmatrix} 0.0746421 & 0 & 0 \\ 0 & 0.0755015 & 0 \\ 0 & 0 & 0.00749571 \end{bmatrix} (kg - m^2).$$

The generalized inertia force due to the physical mass parameters (i.e., hydrodynamic added mass not included yet) of the system can now be computed from (13).

4.4. *Computation of Gravity Forces for Example Model*

The generalized active force due gravity is computed from (14). The result computed from Mathematica for the generalized active force along the direction of the first generalized speed (i.e., v_x) is given by:

$$(F_1)_{\text{grav}} = m_0 g_x + m_1 g_x + m_2 g_x + m_3 g_x,$$

where, g_x is the x component of gravity represented in the 0th coordinate frame.

4.5. *Hydrodynamic Forces for Example Model*

In the absence of experimentally derived hydrodynamic coefficients for an actual vehicle and manipulator, we will make certain assumptions about both the the vehicle and manipulator in order to approximate the hydrodynamic forces for the purposes of simulation. When better data becomes available about a specific URV, it can easily be incorporated into the model and simulation by regenerating the model through Mathematica. However the approximations and model developed here should be adequate for the general study of URV dynamics and control system design.

Added Mass. In general, the motion of a 6 DOF URV moving at high speeds will be highly nonlinear and coupled. However, for many URV applications the URV will be operating at relatively low speeds. With the assumption of a slowly moving URV and 3 planes of symmetry, the off-diagonal elements of the added mass matrix I_A can be neglected (Fossen, 1994). We will model the vehicle as a prolate ellipsoid

$$x^2/a^2 + y^2/b^2 + z^2/b^2 = 1,$$

with semi-major axis "a" along the $\hat{x}_0$ axis and "b" along the $\hat{y}_0$ and $\hat{z}_0$ axes. Define eccentricity e and mass of the water displaced by the spheroid as m as the following:

$$e = 1 - (b/a)^2,$$
$$m = 4/3\pi\rho ab^2.$$

The constants α_0 and β_0 are calculated from:

$$\alpha_0 = \frac{2(1-e^2)}{e^3}\left(\frac{1}{2}\ln\frac{1+e}{1-e} - e\right),$$

$$\beta_0 = \frac{1}{e^2} - \frac{1-e^2}{2e^3}\ln\frac{1+e}{1-e}.$$

Then, the diagonal terms for the vehicle's added mass matrix are given by the following.

$$\mathbf{I}^0_{A_0 11} = -\frac{\alpha_0}{2-\alpha_0}m,$$
$$\mathbf{I}^0_{A_0 22} = -\frac{\beta_0}{2-\beta_0}m,$$
$$\mathbf{I}^0_{A_0 33} = \mathbf{I}^0_{A_0 22},$$
$$\mathbf{I}^0_{A_0 44} = 0.0,$$
$$\mathbf{I}^0_{A_0 55} = -\frac{1}{5}\frac{(b^2-a^2)^2(\alpha_0-\beta_0)}{2(b^2-a^2)+(b^2+a^2)(\beta_0-\alpha_0)}m,$$
$$\mathbf{I}^0_{A_0 66} = \mathbf{I}^0_{A_0 55}.$$

The added mass coefficients for the manipulator will be derived by approximating the links as cylinders. The added mass derived for a cylinder can be found in Patel (1989). We will apply the same assumptions for the links as we did for the vehicle (low speed operation, 3 planes of symmetry) so that off diagonal terms may

again be neglected. Furthermore, we will assume that the added mass contribution due to accelerations along the length of the cylinder axes to be negligible. Thus for a cylinder oriented such that the length of the cylinder is along the $\hat{z}$ axis, the added mass inertia matrix may be approximated as:

$$\mathbf{I}^j_{A_j} = \text{diag}\left\{k_j,\ k_j,\ 0,\ \frac{k_j L_j^2}{3},\ \frac{k_j L_j^2}{3},\ 0\right\},$$

where $k_j = \rho\pi r_j^2 L_j/4$, r_j and L_j are the radius and length of the cylinder. It must be emphasized that although these added mass derivatives are approximations, the dynamic formulation which incorporates them into the equations of motion is based on a general formulation without regard to how the added mass coefficients were derived. When experimental data and/or better model approximations for the added mass parameters become available, it can easily be incorporated into the URV dynamic model and simulation.

Buoyancy Force. The form of the buoyancy force is nearly identical to the force due to gravity except that the force is proportional to the mass of the volume of the displaced fluid instead of the mass of the submerged body. In our simulation model we will assume that the mass of the displaced fluid is equal to the mass of the submerged body so that we can maintain a vertical equilibrium. This is a valid assumption for the vehicle, since underwater vehicles will typically use ballast in order to compensate for the buoyancy force. Variations between the buoyancy and gravity forces on the links of the manipulator will produce a force and a torque on the vehicle, which will increase the station keeping cost of the URV. Careful manipulator design can ensure that the buoyancy and gravity force are nearly equivalent. Therefore, we will nominally model the buoyancy force on the manipulator links as equivalent to the gravity force. We can then introduce variations into the nominal buoyancy force to examine its effect as a disturbance on the URV.

Fluid Acceleration. Fluid acceleration will typically be studied under the context of a model disturbance and will not be incorporated into the example model. The form of the model is equivalent to the gravity and buoyancy force and can be incorporated into the simulation at a future time by simply modifying a routine which computes buoyancy.

Profile Drag. The drag model for the URV will consider separate models for the vehicle and manipulator. The drag on the vehicle will be modeled by approximating the vehicle shape as a sphere with a frontal reference area S_0. The drag and torque induced by the vehicles relative velocity in the fluid is then given by:

$$\mathbf{R}_{\text{Drag}_0} = -1/2 C_{D_0} \rho v_0^2\, S_0,$$
$$\mathbf{T}_{\text{Drag}_0} = 0,$$

where, v_0 is the relative velocity of vehicle with respect to the fluid, and C_{D_0} is the drag coefficient for a sphere.

The drag force exerted on the links of the manipulator will be modeled by approximating the links as cylinders and then applying strip theory. The drag equations become:

$$\mathbf{R}_{\text{Drag}_j} = -0.5\rho \int_0^L \|v_j^0(l)^\perp\| v_j^0(l)^\perp C_D 2 r_j dl,$$

$$\mathbf{T}_{\text{Drag}_j} = -0.5\rho \int_0^L \|v_j^0(l)^\perp\| (\tilde{\mathbf{A}}_0^j l\hat{x}_j \times v_j^0(l)^\perp) \times C_D 2 r_j dl,$$

where r_j is the radius of the cylinder of Link j. A value of $C_{D,\text{basic}} = 1.1$ is suggested by Lévesque and Richard (1994) for a cylindrical cross section. Although the drag models for both the vehicle and the manipulator are approximations, no assumptions were necessary regarding the incorporation of these forces into the dynamic model. The drag force and torque for each element (Link) in the system is represented in the dynamic equations as a symbolic force and torque vector expressed in the 0th coordinate frame, the elements of which are computed by the above approximate equations. Therefore, an improved drag model can easily be incorporated into the dynamic model by replacing the routines which compute the elements of the generic drag force vectors.

5. Summary and Conclusions

The dynamic equations for an underwater vehicle with an n-axis manipulator have been developed using Kane's equations. Kane's method provides a straightforward approach for incorporating external forces into the model. External hydrodynamic forces considered in this model include: buoyancy, profile drag, added mass, fluid acceleration. Other external forces include gravity, manipulator joint torques, and the vehicle's

linear and angular control inputs. The technique was demonstrated for a generic 6DOF vehicle with a 3 link Puma 560 manipulator. The resulting set of dynamic equations are a closed form representation of the complete system and provides the physical insight necessary to study the behavior of the total system. It may be advantageous in future applications to perform coordinated control of both the vehicle and manipulator so that a target point is reached in a prescribed manner. Developing a controller to provide coordinated motion control of the vehicle and manipulator will require an accurate dynamic model which describes the behavior of the total system.

Control of underwater robotic vehicles presents many challenges. Underwater robotic vehicles may exhibit non-holonomic phenomena and may encounter dynamic singularities. Disturbances introduced by the underwater environment are unique. Therefore, control schemes developed for spacecraft robotic systems may be rendered unsuitable by the unstructured underwater environment. The model presented in this paper provides a complete description of the combined motion of a vehicle and manipulator in an underwater environment and will provide the understanding necessary to develop an appropriate control for underwater robotic vehicles. There are still many problems which must be resolved before autonomous underwater robotic vehicles can be successfully deployed. In addition to the problem of vehicle control, underwater robotic vehicles must address problems in the area of: underwater vision, communication, as well as navigation.

Notes

1. The Appendix for this paper is available via the Internet at ftp site, http://www.eng.hawaii.edu/ME/Research/URTC.

References

Angeles, J., Ma, Ou, and Rojas, A. 1989. An algorithm for the inverse dynamics of n-axis general manipulators using Kane's equations. *Computers and Mathematics with Applications*, 17(21):1545–1561.

Craig, J.J. 1989. *Introduction to Robotics*, Addison-Wesley Publishing Company.

Fossen, Thor I. 1994. *Guidance and Control of Ocean Vehicles*, John Wiley & Sons.

Goheen, K.R. 1991. Modeling methods for underwater robotic vehicle dynamics. *Journal of Robotic Systems*, 8(3):295–317.

Goheen, K.R. and Jefferys, E.R. 1990. Multivariable self-tuning autopilots for autonomous and remotely operated underwater vehicles. *IEEE Journal of Oceanic Engineering*, 15(3):144–151.

Healey, A.J., Rock, S.M., Cody, S., Miles, D., and Brown, J.P. 1994. Toward an improved understanding of thruster dynamics for underwater vehicles. *Proceedings of 1994 Symposium on Autonomous Underwater Vehicle Technology*, pp. 340–352.

Ioi, K. and Itoh, K. 1990. Modeling and simulation of an underwater manipulator. *Advanced Robotics*, 4(4):303–317.

Kane, T.R., Likens, P.W., and Levinson, D.A. 1983. *Spacecraft Dynamics*, McGraw-Hill Inc.

Kato, N. and Lane, D.M. 1995. Coordinated control of multiple manipulators in underwater robots. *9th Int. Symposium on Unmanned, Untethered Submersible Technology*, pp. 34–50.

L'evesque, B. and Richard, M.J. 1994. Dynamic analysis of a manipulator in a fluid environment. *The International Journal of Robotics Research*, 13(3):221–231.

Mahesh, H., Yuh, J., and Lakshmi, R. 1991. A coordinated control of an underwater vehicle and robotic manipulator. *Journal of Robotic Systems*, 8(3):339–370.

McMillan, S., Orin, D., and McGhee, R. 1995. Efficient dynamic simulation of an underwater vehicle with a robotic manipulator. In *IEEE Transactions on Systems, Man, and Cybernetics*.

Nakamura, Y. and Savant, S. 1992. Nonlinear tracking control of autonomous underwater vehicles. In *Proceedings of the 1992 IEEE International Conference on Robotics and Automation*, A4–A9.

Patel, M.H. 1989. *Dynamics of Offshore Structures*, Butterworths.

Tarn, T.J., Bejczy, A.K., Marth, G.T., and Ramadorai, A.K. 1991. Kinematic characterization of the PUMA 560 manipulator, Lab Report, SSM-RL-91-15, Dept. of SSM, Washington University, St. Louis.

Whitcomb, L.L. and Yoerger, D.R. 1995. Comparative experiments in the dynamics and model-based control of marine thrusters. In *Proceedings of Oceans'95 MTS/IEEE*, San Diego, CA.

Yoerger, D.R. and Slotine, J.J.E. 1985. Robust trajectory control of underwater vehicles. *IEEE Journal of Oceanic Engineering*, OE-10(4):462–470.

Yoerger, D.R., Cooke, J., and Slotine, J.J.E. 1990. The influence of thruster dynamics on underwater vehicle behavior and their incorporation into control system design. *IEEE Journal of Oceanic Engineering*, 15(3):167–177.

Yuh, J. 1990. Modeling and control of underwater robotic vehicles. In *IEEE Transactions on Systems, Man, and Cybernetics*, 20:531–543.

Yuh, J. 1995. *Underwater Robotic Vehicles: Design and Control*. TSI Press.

Yuh, J. and Gonugunta, K.V. 1993. Learning control of underwater robotic vehicle. *Proceedings of IEEE Int. Conference on R&A*, Atlanta Georgia.

Tzyh-Jong Tarn received the D.Sc. degree in control system engineering from Washington University, St. Louis, MO.

He is at present a Professor in the Department of Systems Science and Mathematics and the Director of the Center for Robotics and Automation at Washington University.

An active member of the IEEE Robotics and Automation Society, Dr. Tarn has served as the President of the IEEE Robotics and Automation Society, 1992–1993. He currently serves as the Chairman of the Nomination Committee of Robotics and Automation Society, the Editor of the IEEE TAB/ Press Book Series on Design and Applications, an Editor of the IEEE/ASME Transactions on Mechatronics, the Director of the IEEE Division X (Systems and Control), and a member of the IEEE Board of Directors. The Japan Foundation for the Promotion of Advanced Automation Technology presented him with the Best Research Article Award in March, 1994. He also is a recipient of the Best Paper Award at the 1995 IEEE/RSJ International Conference on Intelligent Robots and Systems. He is a fellow of The Institute of Electrical and Electronics Engineers, Inc.

Gregg Shoults received a B.S. in Aerospace Engineering from Parks College of St. Louis University, St. Louis, Missouri in 1984, and a M.S. in Aeronautical & Astronautical Engineering from Purdue University, W. Lafeyette, Indiana, in 1987. Mr. Shoults has worked in the Aerospace industry since 1987 in the area of dynamics and control and is presently employed by McDonnell Douglas Aerospace as an Avionics engineer working on the Navy F/A-18 aircraft program. Mr. Shoults is also pursuing a D.Sc. at Washington University in the System Science & Mathematics Department where his research efforts are focused on the dynamics and control of an autonomous underwater robotic vehicle.

Shiaw-Pyng Yang received his B.S. Degree in Physics from Chung-Yuan Christian University in Taiwan in 1988, and M.S. degree in electrical engineering from Northern Illinois University in 1992 and M.S. degree in System Science and Mathematics from Washington University in 1994. Now he is working at the Robotics Laboratory at Washington University while persuing his D.Sc. degree.

His research interests include automatic control, intelligent robotic systems, system design and analysis, and underwater robotic system.